Radial porosity profiles are a powerful tool for tracing locomotor maturation in developing limb bones

Prondvai, Edina; Butler, Richard

DOI:
10.1002/jmor.21567

Document Version
Publisher's PDF, also known as Version of record

Citation for published version (Harvard):
Prondvai, E & Butler, R 2023, 'Radial porosity profiles are a powerful tool for tracing locomotor maturation in developing limb bones', *Journal of Morphology*, vol. 284, no. 4, e21567. https://doi.org/10.1002/jmor.21567

Received: 23 November 2022 | Revised: 30 January 2023 | Accepted: 4 February 2023

DOI: 10.1002/jmor.21567

RESEARCH ARTICLE

JOURNAL OF morphology WILEY

Radial porosity profiles are a powerful tool for tracing locomotor maturation in developing limb bones

Edina Prondvai | Richard J. Butler

School of Geography, Earth & Environmental Sciences, University of Birmingham, Birmingham, UK

Correspondence
Edina Prondvai, School of Geography, Earth & Environmental Sciences, University of Birmingham, Edgbaston, Birmingham, UK.
Email: edina.prondvai@gmail.com and E.Prondvai@bham.ac.uk

Funding information
H2020 Marie Sklodowska-Curie Actions

Abstract

Radial porosity profiles (RPP) are a new quantitative osteohistological parameter designed to capture the dynamic changes in the primary porosity of limb bones through ontogeny, providing insights into skeletal growth and functional development of extant and extinct vertebrates. Previous work hypothesized that RPP channelization—the intraskeletal alignment of RPPs across different bones resulting from similar cortical compaction patterns—indicates increasing locomotor performance of the developing limbs. By investigating RPPs in ontogenetic series of pheasants, pigeons and ducks representing distinct locomotor developmental strategies, we test this hypothesis here and show that RPPs are indeed powerful osteohistological correlates of locomotor ontogeny. Qualitative and quantitative analyses reveal strong association between RPP channelization and fledging, the most drastic locomotor transition in the life history of volant birds. The channelization signal is less clear in precocial leg function; however, when additional intraskeletal and intercohort RPP characteristics are considered, patterns related to leg precocity can also be identified. Thus, we demonstrate that RPPs can be used in future by palaeobiologists to generate breakthroughs in the study of the ontogeny and evolution of flight in fossil birds and pterosaurs. With further baseline data collection from modern terrestrial vertebrates, RPPs could also test hypotheses regarding ontogenetic postural shifts in dinosaurs and other terrestrial archosaurs.

KEYWORDS
birds, fledging, precocial–altricial development, quantitative bone histology, RPP channelization

1 | INTRODUCTION

Parameters of bone histology that can be quantitatively related to biological attributes of vertebrates, such as basal metabolic rate, growth and musculoskeletal function, are fundamental to many studies of extinct species ranging from fossil fish to dinosaurs (e.g., Cubo et al., 2012; Davesne et al., 2018; Kuehn et al., 2019; Lee & Simons, 2015; Legendre et al., 2016; McGuire et al., 2020). Recently, Prondvai et al. (2022) used a preliminary data set to introduce a new osteohistological parameter, referred to as the radial porosity profile (RPP). RPPs quantify the relative changes in primary porosity from the innermost to the outermost cortex in the mid-shaft of limb bones; a histocharacter known to reflect growth dynamics (e.g., Castanet et al., 1996; Cubo & Jalil, 2019; de Buffrénil et al., 2008; de Margerie

et al., 2002; de Margerie et al., 2004; Francillon-Vieillot et al., 1990; Williams et al., 2004).

Prondvai et al. (2022) applied the RPP approach to a small selection of extant and fossil paravians (birds and closely related theropod dinosaurs). They showed that RPPs have versatile analytical potential and identified an apparent correlation with locomotor development during ontogeny. Their preliminary results suggested that the progressive channelization of RPPs, that is the mutual alignment (similar shapes and porosity values) of RPPs of different limb bones within an individual, coincides with the increasing functional performance of the limb modules through ontogeny (Prondvai et al., 2022). These conclusions were largely based on ducks characterized by disparate fore- and hind-limb development (Castanet et al., 1996; Dial & Carrier, 2012; Dial, Tobalske et al., 2012; Prondvai et al., 2020) which represented the most complete, cohort-defined ontogenetic sample in their study.

Based on their findings, the authors hypothesized that RPP channelization indicates the level of functional maturity and hence was proposed as the first quantifiable, standardisable and comparative osteohistological correlate to infer that a limb bone has approached or reached its mature locomotor performance. If this hypothesis is correct, the study of RPPs in a variety of fossil tetrapods would have the potential to shed light on key questions in their locomotor development, such as the onset of flight or ontogenetic postural shifts (Prondvai et al., 2022).

Here, we test this hypothesis by extending the developmental strategy spectrum of our previous preliminary data set that largely relied on ducks with modular limb development. By sampling and analyzing limb bone RPPs of complete ontogenetic series of the highly precocial ring-necked pheasant (*Phasianus colchicus*), the chicks of which fledge at a very early posthatching age, and the highly altricial homing pigeon (*Columba livia*) which only leaves the nest when close to final size, we demonstrate that RPP channelization is indeed a highly reliable indicator of locomotor maturation regardless of whether or not diametric bone growth is still in progress. Other ontogenetically changing characteristics, such as the course of RPPs in homologous bones or the level of skeletal dissociation, are also shown to aid inferences on the limbs' functional performance. These new data on extant birds provide the first firm osteohistological correlate of locomotor development which can therefore be used to advance the detection, identification and hence our understanding of various locomotor ontogenies in long extinct vertebrates.

2 | MATERIALS AND METHODS

2.1 | Material

Pheasants (*Phasianus colchicus* Linnaeus, 1758) were collected from a farm (Pentre Farm, Llangollen) in North Wales during the breeding season in 2020. The sample encompasses a complete ontogenetic series represented by 24 pheasants from posthatching Day 2 up to adulthood, that is, when the animals have reached their maximum body length, are at or close to their mass asymptote and possess a functionally mature plumage. The farm enclosures in which the different pheasant cohorts were grown were large enough for the fledged animals to fly. We only salvaged animals that died of natural causes (accidents or unidentified) within their enclosures, which were monitored daily allowing pheasant carcasses to be collected as freshly as possible. Specimens were weighed and tagged with a note of their age, weight, the possible cause and date of death, and were kept in a freezer until their dissection could be performed at the University of Birmingham.

For pigeons, we used transverse section images of 62 undecalcified histological slides of humeri, ulnae, femora and tibiotarsi of 16 specimens representing a growth series of homing pigeon (*Columba livia forma domestica*), published in the study of McGuire et al. (2020) and made accessible at the Paleohistology Repository (http://paleohistology.appspot.com/Page/Columba_livia.html).

RPP data for ducks (*Anas platyrhynchos domesticus*) published in our previous study (Prondvai et al., 2022) were reused in this analysis.

Table 1 and Supporting Information: Online Materials S1-S4 lists the specimens used in this study with further details on the specimens, their sampled bones and raw measurement data.

2.2 | Dissection and ground section preparation

For the pheasants, we followed the dissection and bone mid-shaft sampling protocol for the humeri, ulnae and carpometacarpals (cmc) of the forelimbs, and femora, tibiotarsi and tarsometatarsi (tmt) of the hind limbs, as described for ducks in Prondvai et al. (2020). Undecalcified bone sample preparation for plastic embedding followed published protocols (Lee & Simons, 2015; McGuire et al., 2020). Plastic-embedded samples were mounted on slides, sectioned, thinned to ~50–70 μm and cover-slipped following Prondvai et al. (2020). Sectioning and grinding steps were performed on a PetroThin Thin Section Machine (Buehler) at the University of Oxford, manual polishing of sections to final thickness was performed at the University of Birmingham.

2.3 | Visualization and RPP measurements

All methodological steps of microscopic investigation, section imaging, histomorphometric measurements and RPP construction were identical with those outlined in Prondvai et al. (2022), here using a Zeiss Axioscope microscope and attached Axiocam 208 color digital camera for visualization of sections, ImageJ 1.53 k (Schneider et al., 2012) to measure porosity in primary cortical bone and Inkscape 0.92.4 (Inkscape Project, 2020) to produce figures. Relative porosity (%) was measured in three section sectors, each constituting four quadrants, Q_a, Q_b, Q_c, and Q_d, that radially equally divide the cortex from the perimedullary to the periosteal region, respectively. Standardized sector assignment

TABLE 1 Details of the pheasant and pigeon specimens used in this study.

Taxon	Specimen ID	Age (dph)	Mass (g)	Sampled bones						Specimen's origin
				Hu	Ul	Cmc	Fe	Ti	Tmt	
Phasianus colchicus	Ph2_13	2	13	■			■	■	■	Pentre Farm, Llangollen, North Wales
	Ph3_26	3	26	■			■	■	■	
	Ph4_14	4	14	■			■		■	
	Ph5_16	5	16	■			■	■	■	
	Ph6_12	6	12				■	■	■	
	Ph10_40	10	40	■	■	■	■	■	■	
	Ph11_46	11	46	■	■	■	■	■	■	
	Ph11_61	11	61	■	■	■	■	■	■	
	Ph20_101	20	101	■	■	■	■	■	■	
	Ph23_93	23	93	■	■	■	■	■	■	
	Ph23_119	23	119	■	■	■	■	■	■	
	Ph31_122	31	122	■	■	■	■	■	■	
	Ph31_142	31	142	■	■	■	■	■	■	
	Ph32_164	32	164	■	■	■	■	■	■	
	Ph41_214	41	214	■	■	■	■	■	■	
	Ph41_215	41	215	■	■	■	■	■	■	
	Ph41_240	41	240	■	■	■	■	■	■	
	Ph49_306	49	306	■	■	■	■	■	■	
	Ph49_393	49	393	■	■	■	■	■	■	
	Ph49_432	49	432	■	■	■	■	■	■	
	Ph94_530	94	530	■	■		■	■	■	
	Ph94_758	94	758	■	■	■	■	■	■	
	Ph112_655	112	655	■	■	■	■	■	■	
	Ph117_1405	117	1405	■	■	■	■	■		
Columba livia	MWU260_1.5	10.5	131	■	■		■	■		Paleohistology Repository (http://paleohistology.appspot.com/Page/Columba_livia.html)
	MWU261_1.5	10.5	83	■	■			■		
	MWU258_2.5	17.5	242	■	■		■	■		
	MWU267_2.5	17.5	263	■	■		■	■		
	MWU269_3.5	24.5	372	■	■		■	■		
	MWU270_3.5	24.5	209	■	■		■	■		
	MWU271_3.5	24.5	209	■	■		■	■		
	MWU272_3.5	24.5	341	■	■		■	■		
	MWU273_4.5	31.5	314	■	■		■	■		
	MWU274_4.5	31.5	374	■	■		■	■		
	MWU275_4.5	31.5	364	■	■		■			
	MWU276_4.5	31.5	360	■	■			■		
	MWU256_5.5	38.5	455	■	■		■	■		
	MWU257_5.5	38.5	498	■	■		■	■		
	MWU254_9	63	482	■	■		■	■		
	MWU255_9	63	563	■	■		■	■		

Note: Light and dark gray fills indicate sampled fore- and hind-limb bones, respectively. For details about the duck specimens see (Prondvai et al., 2022) and Table S4.

Abbreviations: Cmc, carpometacarpus; Fe, femur; Hu, humerus; Ti, tibiotarsus; Tmt, tarsometatarus; Ul, ulna.

was not possible due to ontogenetic and interelemental variability in local cortex thickness, spatial extent of secondary remodeling and general quality of the sections. Instead, sectors were selected to capture the maximum intrasectional diversity in primary porosity patterns. Corresponding quadrant porosities averaged over the three sampling sectors generate a mean 4-point RPP for each bone (Prondvai et al., 2022) (Supporting Information: Table S1-S4).

2.4 | Numeric analyses

After initial qualitative assessment, RPPs were analyzed with a selection of methods based on the apparent ontogenetic patterns recognized. First, we performed principal component analysis (PCA) on the RPPs in each of the three taxa and then on the entire data set to visually explore their arrangement in relation to the age, type of bone, limb, fledging status, and taxonomical assignment of the individuals. The PCA biplot is also a means of detecting skeletal dissociation by showing how spread-out the bones of an individual appear.

We applied two grouping methods to generate objective RPP groups within and across taxa: (1) group-based trajectory modeling (GBTM), which is able to numerically test and select the best supported number of groups in an RPP data set (Nagin, 1999, 2014; Nielsen et al., 2014, 2018); and (2) K-means clustering, which was shown to give the most sensible clustering of RPPs in our previous study (Prondvai et al., 2022). K-means was run with the pre-set cluster numbers that were best supported by GBTM in each taxon separately. We also performed K-means with 2–5 clusters on the entire RPP data set with all three taxa combined, and with 2–4 clusters on the RPPs of homologous elements separately in each taxon. In the latter analyses, GBTM could not be sensibly used due to sample size issues, so we selected the most rational cluster numbers based on the visual inspection of the RPP plots against their color-coded cluster memberships. We focused on the results of the selected cluster numbers to further investigate whether and how group memberships might reflect developmental characteristics. Cluster memberships were also used to determine the level of skeletal dissociation in each individual in relation to its respective developmental state.

As a key aspect of this study is to investigate whether RPP channelization is indeed a good predictor of locomotor maturation of the limbs, the way RPP channelization is quantified and analyzed is of crucial importance. In addition to trajectory grouping methods, analyzing porosity variance within and across RPPs can also capture mutual RPP alignment across bones of an individual or across the cohorts of a species. Because porosity values are percentages ranging from 0 to 100 (between 0 and 1 in ratio form), we used beta regression (Cribari-Neto & Zeileis, 2010) to quantify within- and across-RPP variance. We fitted the intercept-only model with a logit-link function on the porosity values of each bone (within-RPP) and of corresponding quadrants across bones of an individual (across-RPP) and calculated the 68% interquantile ranges of the regression. These 68% prediction intervals represent the variance detected within and across RPPs. Whereas within-RPP variance informs about the course of the RPP, that is, how different or uniform porosity is from the inner to the outer cortex, across-RPP variance is a parameter that captures intraskeletal porosity variation by quantifying how spread out or converging the porosity values are in each corresponding quadrant of an individual's limb bones. Thus, each individual is characterized by four across-RPP variance values (P_a–P_d) and as many within-RPP variance values as sampled bones. For further, visual explanation of RPP variances and their calculations, see Supporting Information: Online Material Figure S1 and Supporting Information: 1.

Variances calculated using these approaches were then compared with 2-sample permutation tests—a nonparametric test that can work with unbalanced sample sizes—between pre and postfledging elements/individuals as well as between forelimb and hind limb bones and combinations of these four categories (Supporting Information: Online Material Tables S5, S6). Within-RPP variance in homologous bones through ontogeny were looked at separately as well. Across-RPP variance was also analyzed against age and the resulting fitted functions were derived at certain age values before, at, and after fledging. The derived slopes were then used to demonstrate how suddenly or gradually across-RPP variance changes with age in the context of precocial-altricial functional development. Finally, because in actively growing specimens, which comprise most of our data set, porosity in the outermost quadrant (Q_d) remains high, P_d can systematically skew within-RPP variance compromising the quantitative detection of RPP channelization that may be apparent in the inner three-quarters of the cortex. Thus, we generated within-RPP variance based only on Q_a, Q_b, and Q_c porosities and ran the analyses on these data sets as well.

In addition to these variance measures, we compared the pre versus postfledging P_d between forelimb and hind limb elements as well as P_d in homologous elements through ontogeny in the context of precocial-altricial functional development.

Given that our duck sample only had a single complete fledgling [50 days posthatching age (dph)] and only two hind limb bones of a postfledging animal, ducks could only be evaluated qualitatively but not statistically in the pre versus postfledging context.

All numeric analyses were implemented in RStudio (1.4.1) integrated development environment (RStudio, PBC) for the free programming language and statistical computing software R (R Core Team, 2020) using the following packages and functions: *prcomp()* and *kmeans()* in basic "stats" for PCA and K-means clustering, *crimCV()* in package "crimCV" (Nielsen, 2018) for GBTM, *betareg()* in package "betareg" (Zeileis et al., 2022) for beta regression, and *permTS()* in package "perm" (Fay, 2015) for 2-sample permutation tests. For detailed R scripts, see Supporting Information: Online Material Information 1.

3 | RESULTS

Because qualitative evaluation and GBTM/K-means analyses of duck RPPs were described in Prondvai et al. (2022), here we focus on pheasants and pigeons in the taxon-specific analyses. However, PCA,

K-means of homologous bones and variance analyses of RPPs, all of which are implemented for the first time in this study, are discussed for all three taxa. For further details of the results, see Supporting Information: Online Material Information 2 and 3.

3.1 | Visual inspection of RPPs

RPP plots imply consistent differences between pre and postfledging individuals in pheasants (Supporting Information: Figure 1a, S2A,) and pigeons (Supporting Information: Figure 1b, S2B,) that largely correspond with the observations made in ducks as they approach fledging age (Supporting Information: Figure 2c, S2C; Prondvai et al., 2022).

In prefledging pheasants (≤14 dph), porosity along the RPPs ranges ~10%–60%, whereas it differs by ~10%–40% in corresponding quadrants among different bones (Figure 1a, Ph2_13 to Ph11_61). Up to 5 dph, the shapes of RPPs appear mostly irregular and independent from one another in each individual, whereas at 10 dph a directional alignment emerges among all bones. Based on the wing bones with enough posthatching cortex to evaluate, no difference in porosity ranges between RPPs of wing and leg elements is evident up to 5 dph, whereas in 10–11 dph specimens, consistently higher porosity levels are seen along RPPs in wing bones than in the leg bones (Supporting Information: Online Material, Figure S2A). By contrast, a strong uniformity appears in the course of RPPs in postfledging animals (Figure 1a, Ph20_102 to Ph117_1405). RPPs

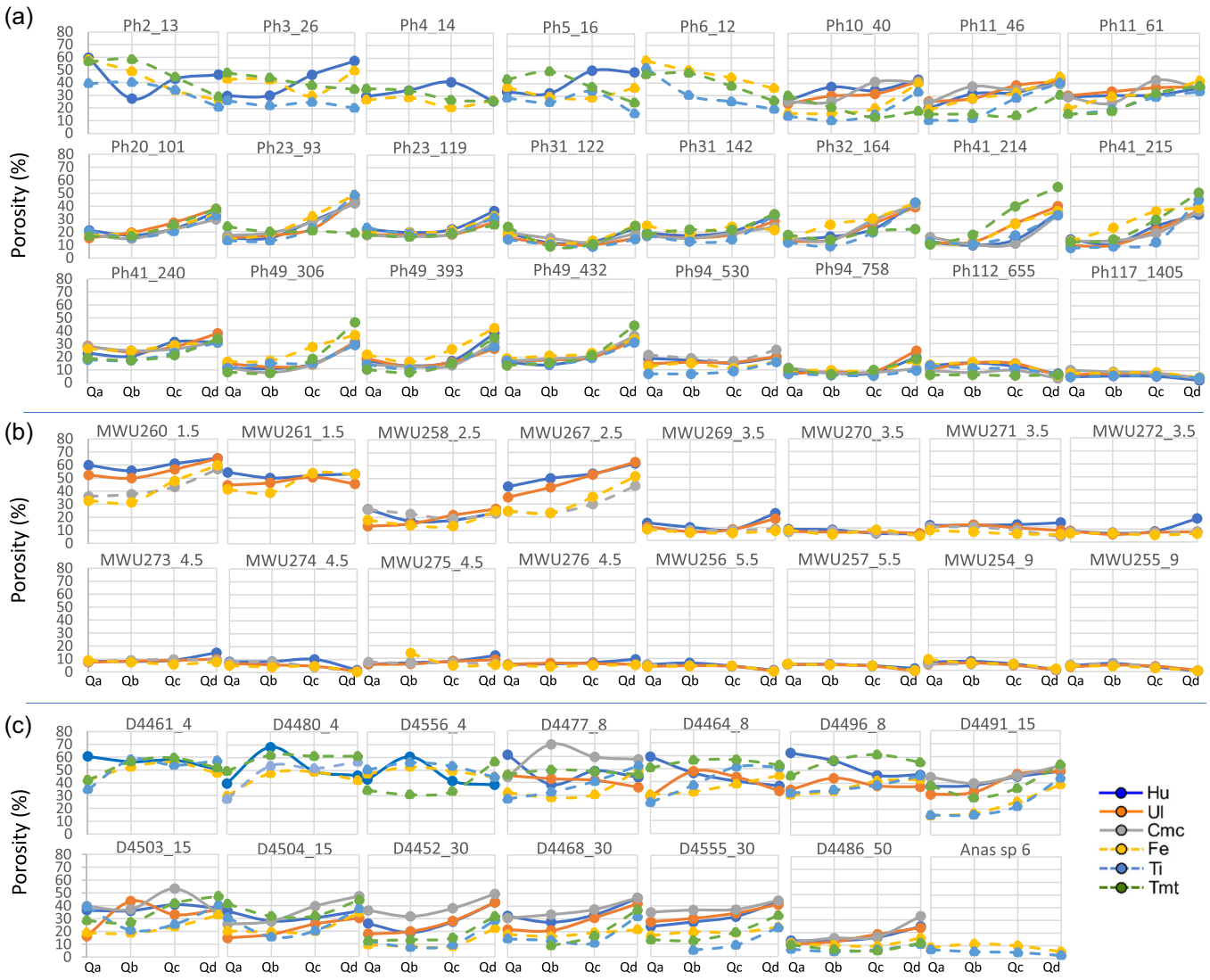

FIGURE 1 Limb RPPs of pheasants (a), pigeons (b) and ducks (c) demonstrating characteristic phases in their respective species-specific locomotor ontogenies. In all three bird species, RPPs show higher porosities, more erratic trajectories and/or less mutual alignment among limb bones in prefledging individuals, while fledging results in RPP channelization and a general drop in porosity. Fledging-related RPP channelization occurs earliest in the precocial pheasants (a) but seems most drastic in the altricially developing pigeons (b). Ducks with precocial leg and altricial wing development show a complex prefledging RPP pattern with a more gradual channelization (c). Note the 2.5 weeks old pigeon specimen MWU 258 treated as "pre-fledging" based on its age shows unusually low porosity and the onset of RPP channelization.

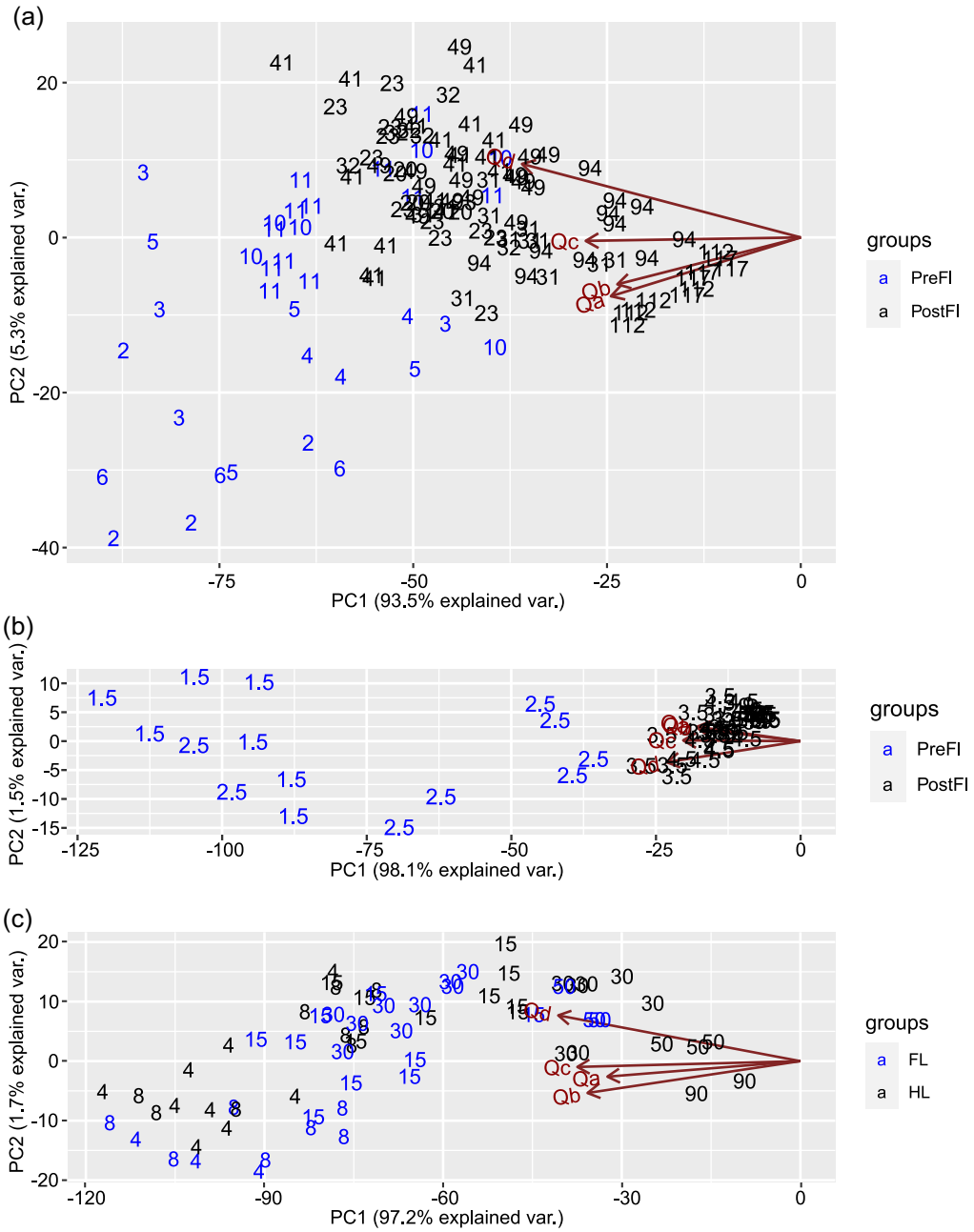

FIGURE 2 PC1-PC2 biplots of limb bone RPPs in pheasants (a), pigeons (b), and ducks (c), color-coded by the grouping factor giving the best RPP separation in the respective taxa. Labels correspond with the age of the sampled individuals (dph in pheasants and ducks; weeks in pigeons). RPPs are best separated by the pre versus postfledging status of the specimens in pheasants (a) and pigeons (b), and by forelimb versus hind limb status (i.e., limb precocity) in ducks (c).

become organized into generally tight, asymmetrical U- or exponential curve-shaped bundles with corresponding quadrant porosities differing only by ~10%–20% and equal porosity ranges for wing and leg bones. This mutual RPP alignment fulfils the criteria of RPP channelization in these postfledging pheasants (Figure 1a). In fully grown specimens (>100 dph, Figure 1a, Ph112_655 to Ph117_1405), porosity drops along the total RPP length with P_d becoming the lowest value coinciding with the formation of an outer circumferential layer (OCL) (Ponton et al., 2004).

In the four prefledging pigeons (≤3 weeks) available for this study, RPPs within an individual show relatively similar shapes with porosity divergence < 30% within corresponding quadrants and no clear difference between forelimb and hind limb porosities (Figure 1b, MWU260_1.5 to MWU267_2.5). Overall RPP porosity levels are high covering ~20%–65%, except in MWU 258 which shows surprisingly low porosity ranges (~10%–30%) (Figure 1b, Supporting Information: S2B). In the postfledging pigeons (≥3 weeks), RPPs of all bones collapse into a single curve with little divergence in porosities of

corresponding quadrants (≤10%; Figure 1b, MWU269_3.5 toM-WU255_9). This represents a striking level of RPP channelization. Porosity drops sharply in all quadrants, and from 4.5 weeks of age, P_d converges on zero corresponding with extensive OCL development (Figure 1b).

Similar trends appear in the ontogenetic changes of RPPs in homologous bones (Supporting Information: Figure S3), in particular regarding outermost cortical porosity (P_d). In the wing bones of prefledging pheasants (Supporting Information: Figure S3A), P_d stays in the highest portion of the ontogenetic P_d range, while in leg bones, P_d occupies the same range in pre and postfledging specimens (Supporting Information: Figure S3A). Interestingly, the wing bones and the femora show a gradually decreasing P_d with age, while there is no apparent trend in the tibiotarsi and tmt at least up to ~50 dph (Supporting Information: Figure S4). This contrasts with the pattern found in ducks where P_d in wing bones shows no clear age-related trend up to 30 dph, while P_d in leg bones gradually decreases with age (Supporting Information: Figure S5).

In the homologous bones of pigeons, RPP porosities are uniformly higher at pre than postfledging ages regardless of the limb (Supporting Information: Figure S3B). Prefledging RPPs show a generally increasing trend, while postfledging RPPs stay flat at nearly constant porosities. P_d steeply declines with age with no difference among elements (Supporting Information: Figure S6).

3.2 | PCA

In the PCA of each of the three taxa, PC1 accounts for >90% variance, the projection of average cortical porosity. In pheasants and pigeons, the best spatial separation of RPPs in the PC1−PC2 biplots is achieved by visualizing the pre versus postfledging status of the bones (Figure 2a,b). All other factors (i.e., bone type, limb, age, specimen) gave more limited or no separation of RPPs (Supporting Information: Figures S7, S8). Although the duck data set could not be evaluated for fledging status, color-coding by limb (i.e., forelimb vs. hind limb) resulted in a good spatial separation in the PC1-PC2 biplot of duck bone RPPs (Figure 2c, Supporting Information: Figure S9). Although age is clearly related to PC1 (Supporting Information: Figure S10), PC1–PC2 biplots seem to reflect the functional performance of the elements rather than their age.

In the PCA of the pooled data set, PC1 accounts for >95% variance. RPPs are best separated by their pre- versus postfledging status on the PC1−PC2 plot (Supporting Information: Figure S11A). A less distinct, partial separation is also identified by taxa (Supporting Information: Figure S11B): in a limited area of the biplot, the elements of ≤30 dph ducks appear to be wedged in between the bones of most prefledging pheasants and all prefledging pigeons, except MWU 258. Neither the bone types, nor the limbs produced clear separation in the PC1−PC2 plot of the pooled data set (Supporting Information: Figure S12). The separation patterns suggest that PC1 and PC2 represent locomotor developmental axes in this pooled data set as well.

3.3 | GBTM and K-means

For the pheasant RPP data set, GBTM (Supporting Information: Figure S13A-C, SI 2) as well as RPP plots color-coded by K-means cluster memberships (Supporting Information: Figure S13D) and cluster compositions showed the best support for the three groups model (Supporting Information: Table S7). The three clusters, respectively, contain (1) all prefledging wing bones but leg bones only up to 6 dph; (2) pre and postfledging leg bones and most postfledging wing bones of actively growing specimens (≤49 dph in our sample); (3) mostly bones of almost or fully-grown animals (Supporting Information: Online Material, SI 3). Skeletal dissociation in the 3-cluster model is low and restricted to prefledging animals (Supporting Information: Table S7).

In pigeons too, the 3-group model was best supported by GBTM (Supporting Information: Figure S14A-C, Supporting Information: Online Material, SI 2) and was also well justified by the RPP cluster compositions and plotted memberships of the 3-cluster K-means analysis (Supporting Information: Figure S14D). However, plotted memberships of the 2-cluster K-means looked equally plausible, although its cluster memberships were surprising: pre and postfledging animals were separated, except the 2.5 weeks old MWU 258 all bones of which were clustered together with those of the postfledging animals. In the 3-cluster K-means, two clusters consist only of prefledging bones, while all the bones of postfledging animals got sorted into a separate cluster (Supporting Information: Table S8, Supporting Information: online material, SI 3). Except for a single prefledging specimen in the 3-cluster setup, K-means, did not dissociate the skeleton of any other pigeon in this sample (Supporting Information: Table S8).

K-means analysis of homologous bones gave similar results in pheasants with three being the most rational group number for all bones, except the tarsometatarsals (Supporting Information: Figure S15A, SI 2). In pigeons, color-coded RPP plots of K-means clusters on homologous bones largely justified 2-3 clusters (Supporting Information: Figure S15B). Except for the femur, all other bones of the 2.5 weeks old MWU 258 at all cluster numbers are separated from the other prefledging bones, either by being assigned to the postfledging cluster, or by forming their own cluster (Supporting Information: Online Material, SI 2, 3).

RPPs of homologous bones in ducks show a more complex pattern. Whereas the color-coded RPP plots of the three forelimb bones clearly indicate which cluster number is the most reasonable, each of the 2−4 clusters of the three hind limb bones seem equally plausible on their respective RPP plots (Supporting Information: Figure S16; Supporting Information: Online Material, SI 2, 3).

K-means analysis of the entire data set gave clues on which bones at which ontogenetic stages show similar RPPs across the three taxa. In this large, multispecies sample, pooled RPPs show gradual change in shape and porosity values which makes visual distinction of potential RPP types difficult. However, five clusters seemed to reflect reasonable RPP groups on the color-coded plots, and hence we chose the 5-cluster K-means as our model to evaluate further (Supporting Information: Figure S17, Table S9).

The composition of three out of the five clusters covers all three taxa, while the other two contain bones only of ducks and pigeons, and of pheasants and ducks, respectively. Once again, cluster compositions imply a complex interspecific pattern of limb bone functional development (Supporting Information: Online Material, SI 2, 3; Table S9).

3.4 | RPP variance (channelization) analyses

Both approaches, within- and across-RPP variance, successfully capture RPP channelization in the context of pre- versus postfledging status and limbs, if porosity in the outermost quadrant (P_d) is considered separately.

Across-RPP variance in all quadrants but Q_d is greater in prefledging than in postfledging animals (Supporting Information: Table S5). Across-RPP variance values against age followed power function in most cases (Supporting Information: Figures S18-20), and with the exception of Q_d in pheasants, the fitted models were significant (Supporting Information: Table S10). Derivatives of all significant power functions show an asymptote phase starting at ~15–20 dph age in pheasants (Supporting Information: Figure S18), and at ~25 dph (3.5 weeks) age in pigeons, before converging on zero (Figure S19). By contrast, in ducks, only the model fitted on the variance in Q_a was statistically significant (Table S10) with derivatives showing an asymptote phase starting ~30 dph (Figure S20). Because of their disparate limb development, we also analyzed across-RPP variance by limbs in ducks (Table S10). Although beta regression was not possible for forelimbs separately because only the humerus was sampled in a few early juveniles, the power function fitted on the across-RPP variance of the hind limbs was significant in all quadrants but Q_c with their derivatives closing the asymptote already at ~8–15 dph (Supporting Information: Figure S21). Details of the functions, model-related statistics and derivates are provided in Supporting Information: 2 and 3.

Within-RPP variance is significantly greater in pre than in postfledging bones and limbs in pigeons, whereas only within-RPP variance calculated without P_d, detected these statistical differences in pheasants. No difference appears in within-RPP variance with or without P_d between forelimb versus hind limb bones in pre and postfledging limbs or when fledging status is not considered (Supporting Information: Table S6). In ducks, only the potential difference in within-RPP variance with or without P_d between fore- and hind-limbs could be tested. Neither of these tests showed difference between fore- and hind-limb bones in ducks through ontogeny (Supporting Information: Table S6).

3.5 | Porosity in Q_d (P_d)

Permutation tests showed that in prefledging pheasants, forelimb bones have higher P_d than hind limb bones, while no difference between limbs is detectable in postfledging animals or when averaged through ontogeny. In ducks, P_d does not differ between wings and legs until fledging age (≤50 dph). In pigeons, while there is no difference in P_d between the limbs in prefledging animals or through ontogeny, postfledging animals show higher P_d in their forelimbs than hind limbs (Supporting Information: Table S11).

In the homologous bones of pheasants, each wing bone showed higher P_d in prefledging than in postfledging animals, while P_d of the three leg bones did not differ between pre and postfledging individuals. By contrast, in pigeons all bones showed higher P_d in prefledging than in postfledging animals (Supporting Information: Table S11). Ducks could not be tested in this context.

4 | DISCUSSION

The qualitative and numeric analyses of limb bone RPPs of pheasants, pigeons and ducks reveal clear consistencies that can be related to their respective locomotor ontogenetic development and that largely support the hypotheses outlined in previous proof-of-concept work (Prondvai et al., 2022). Most importantly, the dynamics of RPP channelization through ontogeny largely correlate with functional development (Figure 3), reflecting the complexity of interactions between growth and locomotor maturation.

4.1 | RPPs as osteohistological correlates of locomotor ontogeny

We consider here two important developmental events in flight-capable birds: the onset of bipedal terrestrial (and potentially arboreal and/or aquatic) locomotion and the onset of flight (i.e., fledging). Even though only three bird species were used in this study, they cover an informative range of developmental strategies on the precocial–altricial spectrum (Figure 3).

Pheasants are on the highly precocial end of the spectrum with hatchlings capable of bipedal locomotion and their wings with flight feathers developing so quickly that chicks are able to fly ~2 weeks after hatching (Myhrvold et al., 2015). Although 2 weeks posthatching in absolute terms may also be long enough for some small bodied, fully altricial passeriform birds to fledge (Myhrvold et al., 2015), these crucial ontogenetic events must be considered in the relative developmental time-frame of the individual species. From hatching, pheasants need ~100 days to reach adulthood (defined here as termination of longitudinal bone growth, approach of the mass asymptote and display of a fully mature plumage). This means that pheasant chicks fledge at ~15% of adult age by which time they have achieved only ~50% of adult bone length and ~10% of adult mass (Supporting Information: Figures S22A, S23A). This level of aerial locomotor precocity among extant birds is surpassed only by megapodes, the chicks of which hatch with fully functional wings (Starck, 1993; Starck & Ricklefs, 1998; Starck & Sutter, 2000).

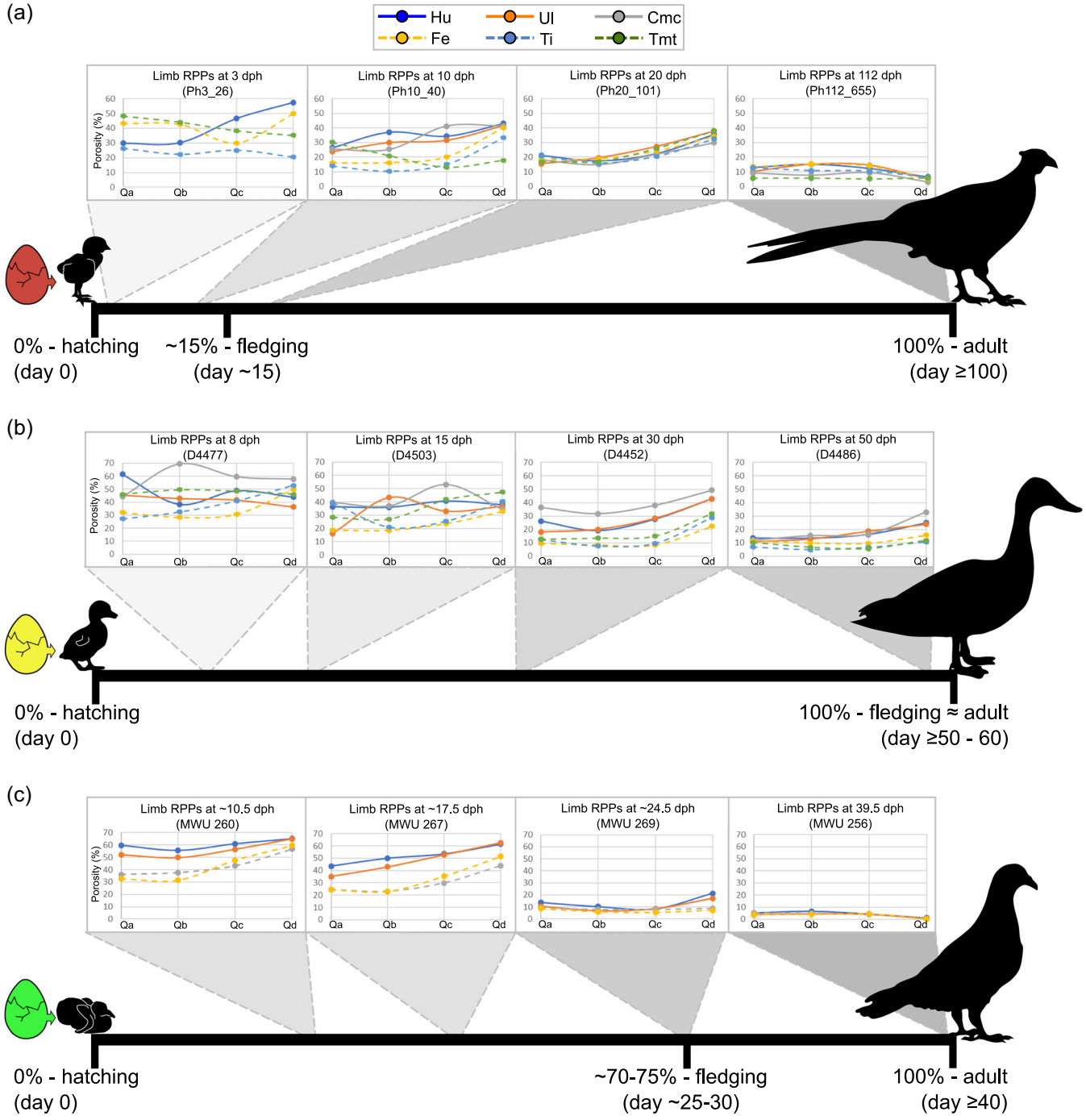

FIGURE 3 Comparative ontogenetic changes in the RPPs of limb bones in three birds with different locomotor ontogenetic strategies. The species-specific ontogenetic trajectories represent the standardized developmental time it takes to reach adulthood (as defined in text). (a), Pheasants hatch with precocial legs and with wings able to perform flight at ~15% of their development (fledging). (b), Ducks hatch with precocial legs but altricial wings and fledge only when they reach adulthood. (c), Pigeons develop fully altricially and fledge at ~70%–75% of their developmental time. Irrespective of its relative ontogenetic timing, in each species fledging is associated with RPP channelization. Note that corresponding RPP patterns related to different phases of locomotor development can also be identified across the three taxa (degree of gray shades) demonstrating the RPPs' potential to be used as a standardized indicator of the locomotor performance along the spectrum of ontogenetic strategies in interspecific comparisons.

Although generally considered precocial, ducks represent a mixed locomotor developmental strategy with legs performing terrestrial and aquatic locomotion from hatching, but wings not ready for flight until close to adulthood (as defined above). In other words, legs develop precocially but wings develop altricially in ducks, contrasting with the overall precocial condition with only a short delay in the onset of flight seen in pheasants. This strong modularity in duck limb functional development is evident in the differing

longitudinal growth dynamics of the wing and leg elements (Dial & Carrier, 2012). Whereas leg bones reach adult length already at 30 dph, wing bones reach their final length only by fledging that occurs at ~50–60 dph. By fledging, longitudinal growth in ducks is completed (Supporting Information: Figure S22B) and they are almost fully grown having reached ~85% of adult mass (Dial & Carrier, 2012).

Pigeons are the most altricial representative of our sample with neither terrestrial/arboreal nor aerial locomotion performed until late in their ontogeny, close to adulthood. Their fledging coincides with leaving the nest, thus sharply contrasting with the precocial pheasants and ducks which leave the nest soon after hatching. Relative mobility of the nest-bound chicks is restricted, and hence functional demands on the limbs are mostly related to positioning, displacing and scrambling movements among the nestlings with progressively increasing frequency of exercises performed as fledging approaches; similar to that documented in other birds (Liang et al., 2018; Ruaux et al., 2020; Thorsen et al., 2004; Yoda et al., 2017 and refs therein). Fledging clearly represents the most abrupt transition in the life history of altricial birds (e.g., Martin et al., 2018; Michaud & Leonard, 2000; Naef-Daenzer & Grüebler, 2016) and hence is expected to be accompanied by the most radical changes in their locomotor systems. In pigeons, fledging occurs at ~25–30 dph which is ~70%–75% of their total developmental period (~40 dph). By this time, >85% of the longitudinal bone growth is achieved (Supporting Information: Figure S22C), but only ~60%–70% of adult mass (McGuire et al., 2020), so considerable mass accumulation continues until ≥40 dph (Supporting Information: Figure S23B).

Put in their respective developmental contexts, the relative timing of RPP channelization in the limb bones of these three taxa reflects the combination of growth and increasing functional demands related to increasing locomotor activity.

Visually, pheasant limb bones start showing the first signs of RPP channelization by 10 dph, with the trend of mutual RPP alignment and dropping porosity levels. In this period before fledging, wing bones show higher porosities than leg bones consistent with their relatively delayed functional deployment. However, although legs perform locomotor functions right after hatching, while wings do not until fledging, no disparate RPP trend appears between fore- and hind-limb bones in <6 dph specimens (Figure 1a, Supporting Information: Figure S2A). Even though this observation is exclusively based on humeri (posthatching cortex in other wing bones is too underdeveloped at ≤6 dph for RPP generation), a similar lack of difference between RPPs of precocial leg bones and altricial wing bones was observed in the youngest ducklings up to 8 dph (Figure 1c, Supporting Information: Figure S2C). This consistency across taxa also supports the hypothesis that the locomotion-induced osteonal compaction lags behind the rapid volumetric cortical expansion in these early ontogenetic stages of fast-growing birds (Prondvai et al., 2022). Furthermore, the underdeveloped posthatching cortex in wing bones is also a strong qualitative indicator of disparate wing and leg development, and hence should be considered in RPP evaluations.

Nevertheless, RPP correlates of precocity in these early prefledging stages can still be identified in homologous bones through ontogeny (Supporting Information: Figures S3-S6). Osteonal compaction is clearly related to functional maturation, and in prefledging pheasants, the leg bones show the same porosity (or compaction) levels in the outer cortical half as their postfledging homologs. By contrast, prefledging wing bones have consistently higher porosity throughout the cortex compared with their postfledging counterparts (Supporting Information: Figures S3A, S4). In ducks, the pattern between wing and leg bones is different but it also concerns the outer half of the cortex. Compaction of the outermost cortex happens in a stepwise manner through ontogeny in the precocial leg bones, while in the altricial wing bones it seems to increase more abruptly right before fledging (Supporting Information: Figures S3C, S5). This suggests that relative compaction of limb bone cortices is driven by the onset of their respective locomotor function, and hence can be used as an additional indicator of locomotor transitions.

By the earliest postfledging age present in our pheasant sample (20 dph), wing and leg bones show the same level of RPP channelization; a pattern implying equally functional fore- and hind-limbs. This channelization is characterized by bundles of wing and leg bone RPPs showing similar shapes and porosity ranges, that is, similar cortical compaction patterns (Figure 1a, Supporting Information: Figure S2A). Lacking postfledging wing bones in our duck sample, no equivalent RPP bundles could be identified in ducks. However, it is clear that up to fledging age (~50 dph), the RPPs of precocial leg bones tend to run below the RPPs of altricial wing bones in ducklings, even though both limbs have similarly shaped RPPs already at 30 dph (Figure 1c, Supporting Information: Figure S2C). The RPP pattern at 30 and 50 dph in ducks resembles that observed in pheasants at 10–11 dph; each taxon being in their respective preparation period for fledging. The progressive RPP alignment and channelization before fledging in both taxa indicates that RPPs can identify corresponding locomotor developmental stages across taxa with different ontogenetic strategies (Figure 3a,b).

The situation in pigeons is less clear due to the low prefledging ontogenetic resolution of our sample with only four specimens representing two, roughly estimated age categories. Considering the relative suddenness of the onset of effective locomotion in the nest-bound pigeons as compared to the precocial pheasants and ducks, differences in the dynamics of RPP changes related to fledging might be expected. However, the postfledging pigeon RPPs indicate that a strong channelization must occur before or at fledging (Figure 3c, Supporting Information: Figure S2B).

The postfledging RPP pattern is also informative of respective developmental strategies. The early flying pheasant chicks still have a great deal of growth ahead of them before reaching adult dimensions. Accordingly, their outermost cortex (Q_d) maintains high porosity, while the bulk of the cortex is much more compacted giving their RPP bundles the asymmetrical U-shape or exponential function shape described above (Figures 1a and 3a, Supporting Information: Figure S2A). By contrast, the radical collapse of RPPs into a quasi-single curve observed around or shortly after fledging (at 3.5 weeks) in pigeons (Figures 1b and 3c, Supporting Information: Figure S2B), where

Q_d shows porosity levels only slightly higher than, equal with, or even lower than the rest of the cortex (Supporting Information: Figures S3B, S6), is in line with their strategy to grow closer to adult size before fledging. Although no postfledging wing bones were available in our duck sample, the low porosity of RPPs, especially in the weight-bearing hind limbs, around fledging age (50 dph) compared to prefledging RPPs suggests that the bulk of growth is indeed completed by fledging (Figure 1c, Supporting Information: Figure s2c). After fledging, further RPP channelization of wing and leg bones via uniformly extensive cortical compaction is expected to soon lead to the same RPP pattern as found in the two hind limb elements of the adult duck. If the latter inference is correct, RPPs through ontogeny reliably reflect the well-known developmental strategy of ducks, as well (Figure 3).

4.2 | Quantitative support for RPP patterns

Results of the variance analyses of RPPs performed to quantitatively capture RPP channelization are in accordance with the qualitatively identified patterns, and hence largely support the above conclusions. Across-RPP variance describing intraskeletal porosity variation in corresponding quadrants among different limb bones is expected to decrease in specimens with channelized limb bone RPPs. This, in turn, is expected to coincide with intensifying functional demands and increasing locomotor performance. Indeed, this is precisely what we found in pheasants and pigeons: across-RPP variance was greater in prefledging than in postfledging individuals in all quadrants, except in Q_d representing the outermost cortex that was still growing in most of our sampled specimens. The sudden drop in across-RPP variance derivatives also coincides with the fledging age in both taxa further supporting the usefulness of this parameter for numerical exploration of RPPs. On the other hand, the fitted models could not sufficiently describe the across-RPP variance pattern in our duck sample which in essence consisted of prefledging individuals, and hence lacked the drastic RPP channelization observed in the other two taxa. However, the separately analyzed hind limb across-RPP variance derivatives reaching an asymptote at ~8–15 dph likely represent the prelude of locomotion-related RPP channelization in the ducklings' precocial legs.

Within-RPP variance, which demonstrates how even or uneven porosity/compaction levels are throughout the cortex, is sensitive to single-point outliers, and hence could not detect RPP channelization in actively growing postfledging pheasant bones with high porosity in Q_d. However, P_d excluded, within-RPP variance also became a reliable parameter to distinguish pre from postfledging animals with high confidence. Still, within-RPP variance was unable to differentiate between altricial forelimb and precocial hind limb RPPs in ducks indicating that prefledging RPPs can have similar shapes regardless of the locomotor performance of the duckling limbs.

PCA visualization and clustering/grouping of RPPs also support the results and interpretations of the qualitative and quantitative analyses of RPP channelization (Figure 2, Supporting Information: Figure S7-9). The bones' spatial arrangement along the first two PCA axes, the K-means cluster compositions, and the skeletal dissociation levels (Supporting Information: Tables S7, S8, S12) are largely consistent with the respective ontogenetic locomotor development of the three avian taxa. Whereas in pheasants and pigeons, the major divisions correspond with the fledging status of the animals, in our largely prefledging duck sample the level of limb precocity appears to be the dominant bone separating factor (Figure 2). Accordingly, K-means-based skeletal dissociation of the animals is highest in ducks and lowest in pigeons, whereas pheasants with slightly more precocial legs than wings show moderate dissociation levels (Supporting Information: Tables S7, S8, S12). In addition, K-means was also able to capture the precocial hind limb condition in pheasants by clustering ≥ 10 dph leg bones together with postfledging bones, and thus separating them from all prefledging wing elements (Supporting Information: Table S7). However, in congruence with all other analyses, K-means could not detect precocity in leg bone RPPs in ≤6 dph pheasant chicks.

The PCA and K-means analyses of the pooled data set gave interesting insights into the potentially corresponding phases of functional development of limb bones across the three taxa. Whereas fledging status was clearly the best separator on the PC1-PC2 plot (Supporting Information: Figure S11A), the projection of the taxonomic assignment seems to reflect the intermediate developmental strategy of ducks between the whole-precocial pheasants and the whole-altricial pigeons (Supporting Information: Figure S11B). As this pattern could best be captured in the respective prefledging ontogenetic stages of the taxa, it supports, once again, the universal RPP channelization effect of fledging. Similarly, K-means cluster memberships imply an intermediate developmental position of ducks between pheasants and pigeons (Supporting Information: Table S9).

Finally, relative porosity in the outermost cortex (Q_d) seems to reflect the temporal difference in the onset of wing- versus leg-driven locomotion in pheasants. P_d is higher in prefledging wing bones than leg bones, while this difference disappears after fledging. Furthermore, prefledging wing bones show higher P_d than their postfledging homologs, whereas no such difference exists between pre and postfledging leg bone homologs. This pattern suggests that difference in the relative porosity of the outermost cortex between the limbs indicates difference in their functional performance. Thus, lower P_d in the legs of pheasant chicks in the prefledging developmental phase is likely related to the leg-driven precocial locomotion from hatching.

In accordance with this hypothesis, pigeons in which prefledging wings and legs equally lack locomotor function show no difference in their P_d. However, after fledging, wing bones show somewhat higher P_d than leg bones. This might be attributed to the predominantly terrestrial/arboreal locomotion of the fledglings: even though they leave the nest, in the first few days, fledgling pigeons tend to stay on the ground or perch on branches and only take short flights if necessary (Liang et al., 2018). This difference between effective functional demand placed on fledgling wing and leg bones may be related to the slight difference in their P_d values. Thus, the ontogenetic timing of emergence and disappearance of potential differences in P_d between the wings and legs could also be used to tackle the development of locomotion.

Interestingly, this pattern does not hold true of ducks which, despite the tremendous difference between prefledging wing and leg functional development, showed no statistically supported difference in their P_d values. A clear difference only appears in ducklings by 30 dph and still exists at 50 dph with the wing bones showing higher P_d than leg bones; however, this age subsample was too small for statistical analysis. The lack of limb separation in earlier ontogenetic stages is a peculiar feature in ducks and awaits further testing.

4.3 | RPPs reveal individual variation

Taken together, all these independent RPP evaluation techniques lead to the convergent conclusion that RPPs are shaped by the complex interactions between growth and function and that RPP characteristics are reliable indicators of relative functional maturity and limb performance.

The analytical power of RPPs is unequivocally demonstrated in the ~2.5 weeks old pigeon specimen MWU 258. Even though its roughly estimated age would suggest a prefledging condition—and accordingly it was considered as such in all of our analyses—its RPPs showed curious indication of ongoing RPP channelization (Figure 1b, MWU258_2.5). This was also reflected in its bones being positioned in the postfledging PCA point cloud of the pooled data set (Supporting Information: Figure S11), clustered together with those of postfledging animals or forming their own single-member clusters in the K-means analyses (Supporting Information: Table S8, SI 2,3). This peculiarity is explained by a surprising level of individual variance in fledging age: despite 2.5 weeks being generally regarded as prefledging age in pigeons, this particular specimen exhibited a fully developed fledging plumage at the time of its death. By sharp contrast, MWU 267, the other specimen of the same ~2.5 weeks cohort, which even had slightly greater body mass than MWU 258, still possessed underdeveloped pin feathers and bald areas on its body surface. This example clearly shows that RPP is able to detect fledging in an age-independent manner.

The considerable inter- and intraspecific fledging time diversity in altricial birds is driven by a variety of factors, such as sibling interactions (Nilsson & Svensson, 1993; Santema et al., 2021), nestling development (Michaud & Leonard, 2000), parent-offspring conflict (Jones et al., 2020), nest predation pressure (Martin et al., 2018; Martin, 2015; Remeŝ & Martin, 2002) and other intrinsic and environmental constraints (Cooney et al., 2020), and similar diversity is expected in the fledging age in precocial birds. Therefore, RPPs are particularly important as an age-independent analytical tool in palaeohistological studies aiming to explore locomotor ontogeny in fossils by means of quantitative bone tissue characteristics.

4.4 | Future directions

With a total of 264 measured and analyzed limb bones of growth series of three avian taxa, our study is the most extensive quantitative ontogenetic osteohistological study of extant birds to date. Yet, there are several aspects of the relationship between RPPs and locomotor developmental characteristics that could not be covered here and need to be explored further. Filling these knowledge gaps by expanding RPP research in modern animals is especially important for studying extinct tetrapods if the RPP method is to be reliably used as the osteohistological correlate of a range of locomotor ontogenetic strategies.

For instance, due to the unbalanced nature of the ontogenetic representation in our sample, the resolution in some crucial locomotor developmental phases was barely or not enough for robust statistical testing. The sample size of pre versus postfledging specimens was uneven within and across the three taxa, and the age estimation in pigeons was relatively crude. Furthermore, even though the pigeon specimen MWU 258 is an evident example of individual variation in growth strategy and functional development, our cohorts did not have enough specimens to statistically address the extent of intraspecific variation. Thus, a better-balanced sample with enough representatives of important stages in ontogenetic locomotor transitions would produce firmer analytical results and a more profound understanding of the processes shaping the RPPs. Nevertheless, intraspecific variability remains hard to assess as it would require a fairly large sample size in each cohort that is usually difficult to acquire.

Besides uniformly indicating crucial developmental events, such as fledging, RPPs also show species-specific characteristics. Among the developmental strategies represented by our three taxa, the disparate limb development in ducks appears to result in the most complex prefledging RPP patterns that are, as a consequence, also the hardest to interpret. A further complication with regard to ducks is their aquatic lifestyle from hatching on. Although both the duck and pheasant hatchlings have precocial hind limbs, the foot-propelled swimming combined with occasional walking/running on land in ducklings and the predominantly terrestrial locomotion with constant weight bearing in pheasant chicks means different centers of mass and gait, and different loading regimes in their hind limbs (e.g., Habib & Ruff, 2008; Hinić-Frlog & Motani, 2010; Wei & Zhang, 2021; Zeffer et al., 2003). Such lifestyle-related differences are likely to affect hind limb bone RPPs throughout ontogeny in as yet unknown ways. Thus, RPP data collection in other taxa with disparate limb development and diverse lifestyles could give a deeper understanding of how these factors influence RPPs as osteohistological indicators of locomotor performance.

Fledging is a key transition in the ontogeny of volant birds; one that leads to the most energy-demanding type of locomotion with systemic effects on the physiology of the whole organism (Scanes, 2014). As such, it is not surprising that the onset of flight has the most radical effect on RPPs through bird ontogeny. By contrast, the onset of terrestrial/aquatic locomotion in precocial birds leaves a much less prominent signal in the hind limb bone RPPs, even if the delayed osteonal compaction relative to volumetric expansion of the posthatching cortex is accounted for. Prefledging RPP channelization in the precocial leg bones is not as distinct as in

postfledging states, and hence the prediction power of RPPs seems lower for early hind limb locomotor function, or the underlying pattern is not yet fully understood due to insufficient data. However, the strong RPP channelization revealed in the semiprecocial juvenile hoatzins (Prondvai et al., 2022) which perform a peculiar wing- and leg-assisted arboreal and aquatic locomotion long before fledging (Abourachid et al., 2019) suggests that the functional deployment of both limbs may be key for obvious RPP channelization to occur. This would imply that not only fledging but the systemic effect of other types of locomotion performed by both limbs likely results in distinct RPP channelization.

Future studies using RPPs to reconstruct changes in terrestrial locomotor development, such as ontogenetic postural shifts, in fossil tetrapods need to consider the current limitation of understanding and be prudent in interpretations. On the other hand, long standing disputes and widely accepted views about the precocial flight capabilities of pterosaur hatchlings (Unwin & Deeming, 2019; Wang et al., 2017) and fossil paravians (Chinsamy & Elzanowski, 2001; Elzanowski, 1981; Varricchio et al., 2015; Xing et al., 2017; Zhou & Zhang, 2004), respectively, could already be osteohistologically addressed and resolved with RPP analysis of early juvenile limb bones. Nevertheless, it remains essential to expand RPP studies to a wider variety of extant volant and nonvolant vertebrates to get a comprehensive understanding of how the many different intrinsic and extrinsic factors might influence RPP patterns through ontogeny.

5 | CONCLUSION

RPP is the first quantitative osteohistological method that is verified on extant birds to yield reliable information on locomotor ontogeny. RPP channelization—the increasing and more or less even compaction of the inner half to three quarters of the primary cortex resulting in the mutual alignment of RPPs among the animal's limb bones—is identified as the osteohistological correlate of functional maturation of the locomotor system. Based on our sample, the onset of flight results in the most obvious RPP channelization in volant birds. In the functionally mature birds with full flight potential, RPP channelization eventually progresses into uniformly low porosity (i.e., high compaction) throughout the cortex, and with the formation of an OCL, this cortical portion becomes effectively avascular. Even though a certain level of RPP channelization also characterizes the onset of terrestrial/aquatic locomotor function in the hind limbs, the signal is less clear and needs further examination. However, the distinct RPP channelization found in the semiprecocial hoatzin chicks that climb and swim with all four limbs way before they start flying suggests that equally developed locomotor function in both limbs may be the key inducer of systemic RPP channelization.

With these findings in modern birds with known locomotor developmental strategies, this study represents a strong foundation for studying the evolution of flight in long extinct volant vertebrates, including key transitional taxa along the dinosaur–bird lineage and pterosaurs, the first actively flying vertebrates in Earth's history. Finally, by adding new RPP data of flightless birds and terrestrial mammals, the range of the diverse ontogenetic information that can be drawn from primary bone tissue as demonstrated here could be extended beyond volancy. This would be crucial for answering long standing questions about quadrupedal versus bipedal ontogenetic postural shifts in a variety of fossil archosaurs; a developmental phenomenon that has no analogs among modern vertebrates.

ACKNOWLEDGMENTS

We are grateful to David Edwards for donating us the dead pheasants from his farm, including monitoring, collecting, storing and recording data of each specimen; Steve and James Butler for general help with arranging access to and temporary storage of pheasant specimens; Matthew Beverley-Smith for extensive help with the sectioning and grinding of bone samples performed at the University of Oxford; Andrew Lee for consultation on plastic-embedding methodology and on the feather development of their pigeon individuals as well as for his meticulous review and help with beta regression analyses; Ivan Sansom, Bethan Phillips and Eimear Orgill for logistic and technical arrangements in the laboratory of the University of Birmingham; Zs. Szovák for help with data organization.

This work was supported by Horizon Europe: Marie Skłodowska-Curie Actions (grant number 882758).

DATA AVAILABILITY STATEMENT

The data that supports the findings of this study are available in the Supporting Information Material of this article.

ORCID

Edina Prondvai http://orcid.org/0000-0002-1284-8311

REFERENCES

Abourachid, A., Herrel, A., Decamps, T., Pages, F., Fabre, A.-C., Van Hoorebeke, L., Adriaens, D., & Garcia Amado, M. A. (2019). Hoatzin nestling locomotion: Acquisition of quadrupedal limb coordination in birds. *Science Advances*, *5*, eaat0787.

de Buffrénil, V., Houssaye, A., & Böhme, W. (2008). Bone vascular supply in monitor lizards (Squamata: Varanidae): Influence of size, growth, and phylogeny. *Journal of Morphology*, *269*(5), 533–543.

Castanet, J., Grandin, A., Abourachid, A., & de Ricqlès, A. (1996). [Expression of growth dynamic in the structure of periosteal bone in *Anas platyrhynchos*]. *Comptes rendus de l'Academie des sciences. Serie III, Sciences de la vie*, *319*, 301–308.

Chinsamy, A. & Elzanowski, A. (2001). Evolution of growth pattern in birds. *Nature*, *412*(6845), 402–403.

Cooney, C. R., Sheard, C., Clark, A. D., Healy, S. D., Liker, A., Street, S. E., Troisi, C. A., Thomas, G. H., Székely, T., Hemmings, N., & Wright, A. E. (2020). Ecology and allometry predict the evolution of avian developmental durations. *Nature Communications*, *11*(1), 2383.

Cribari-Neto, F. & Zeileis, A. (2010). Beta regression in R. *Journal of Statistical Software*, *34*(2), 1–24.

Cubo, J. & Jalil, N. E. (2019). Bone histology of *Azendohsaurus laaroussii*: implications for the evolution of thermometabolism in archosauromorpha. *Paleobiology*, *45*(02), 317–330.

Cubo, J., Le Roy, N., Martinez-Maza, C., & Montes, L. (2012). Paleohistological estimation of bone growth rate in extinct archosaurs. *Paleobiology*, *38*(2), 335–349.

Davesne, D., Meunier, F. J., Friedman, M., Benson, R. B. J., & Otero, O. (2018). Histology of the endothermic opah (*Lampris* sp.) suggests a new structure–function relationship in teleost fish bone. *Biology Letters*, *14*, 20180270.

Dial, T. R. & Carrier, D. R. (2012). Precocial hindlimbs and altricial forelimbs: partitioning ontogenetic strategies in Mallard ducks (*Anas platyrhynchos*). *Journal of Experimental Biology*, *1*, jeb.057380.

Dial, T. R., Tobalske, B. W., & Heers, A. M. (2012). Ontogeny of aerodynamics in Mallard ducks: comparative performance and developmental implications. *Journal of Experimental Biology*, *1*, jeb.062018.

Elzanowski, A. (1981). Embryonic bird skeletons from the late cretaceous of Mongolia. *Palaeontologia Polonica*, *42*, 147–179.

Fay, M. (2015). *Package 'perm': Exact or asymptotic permutation tests*. https://CRAN.R-project.org/package=perm

Francillon-Vieillot, H., Buffrénil, V. D., Castanet, J., Géraudie, J., Meunier, F. J., Sire, J. Y., Zylberberg, L., & De Ricqlès, A. (1990). Microstructure and mineralization of vertebrate skeletal tissues. In J. G. Carter (Ed.), *Skeletal Biomineralization: Patterns, Processes and Evolutionary Trends* (pp. 471–530). Van Nostrand Reinhold.

Habib, M. B. & Ruff, C. B. (2008). The effects of locomotion on the structural characteristics of avian limb bones. *Zoological Journal of the Linnean Society*, *153*(3), 601–624.

Hinić-Frlog, S. & Motani, R. (2010). Relationship between osteology and aquatic locomotion in birds: determining modes of locomotion in extinct ornithurae. *Journal of Evolutionary Biology*, *23*(2), 372–385.

Inkscape Project. (2020). *Inkscape*. https://inkscape.org.

Jones, T. M., Brawn, J. D., Ausprey, I. J., Vitz, A. C., Rodewald, A. D., Raybuck, D. W., Boves, T. J., Fiss, C. J., McNeil, D. J., Stoleson, S. H., Larkin, J. L., Cox, W. A., Schwarzer, A. C., Horsley, N. P., Trumbo, E. M., & Ward, M. P. (2020). Parental benefits and offspring costs reflect parent–offspring conflict over the age of fledging among songbirds. *Proceedings of the National Academy of Sciences*, *117*(48), 30539–30546.

Kuehn, A. L., Lee, A. H., Main, R. P., & Simons, E. L. R. (2019). The effects of growth rate and biomechanical loading on bone laminarity within the emu skeleton. *PeerJ*, *7*, e7616.

Lee, A. H. & Simons, E. L. R. (2015). Wing bone laminarity is not an adaptation for torsional resistance in bats. *PeerJ*, *3*, e823.

Legendre, L. J., Guénard, G., Botha-Brink, J., & Cubo, J. (2016). Palaeohistological evidence for ancestral high metabolic rate in archosaurs. *Systematic Biology*, *65*(6), 989–996.

Liang, X., Yu, J., Wang, H., & Zhang, Z. (2018). Post-Hatching growth of the pectoralis muscle in pigeon and its functional implications. *The Anatomical Record*, *301*, 1564–1569.

Linnaeus, C. (1758). *Systema naturae*. (10th Ed). Tomus I. Stockholm.

de Margerie, E., Cubo, J., & Castanet, J. (2002). Bone typology and growth rate: testing and quantifying "Amprino's rule" in the mallard (*Anas platyrhynchos*). *Comptes Rendus Biologies*, *325*, 221–230.

de Margerie, E., Robin, J.-P., Verrier, D., Cubo, J., Groscolas, R., & Castanet, J. (2004). Assessing a relationship between bone microstructure and growth rate: a fluorescent labelling study in the king penguin chick (*Aptenodytes patagonicus*). *Journal of Experimental Biology*, *207*, 869–879.

Martin, T. E. (2015). Age-related mortality explains life history strategies of tropical and temperate songbirds. *Science*, *349*(6251), 966–970.

Martin, T. E., Tobalske, B., Riordan, M. M., Case, S. B., & Dial, K. P. (2018). Age and performance at fledging are a cause and consequence of juvenile mortality between life stages. *Science Advances*, *4*(6), eaar1988.

McGuire, R. S., Ourfalian, R., Ezell, K., & Lee, A. H. (2020). Development of limb bone laminarity in the homing pigeon (*Columba livia*). *PeerJ*, *8*, e9878.

Michaud, T. & Leonard, M. (2000). The role of development, parental behavior, and nestmate competition in fledging of nestling tree swallows. *The Auk*, *117*(4), 996–1002.

Myhrvold, N. P., Baldridge, E., Chan, B., Sivam, D., Freeman, D. L., & Ernest, S. K. M. (2015). An amniote life-history database to perform comparative analyses with birds, mammals, and reptiles. *Ecology*, *96*(11), 3109.

Naef-Daenzer, B., & Grüebler, M. U. (2016). Post-fledging survival of altricial birds: ecological determinants and adaptation. *Journal of Field Ornithology*, *87*(3), 227–250.

Nagin, D. S. (1999). Analyzing developmental trajectories: A semiparametric, group-based approach. *Psychological Methods*, *4*, 139–157.

Nagin, D. S. (2014). Group-based trajectory modeling: An overview. *Annals of Nutrition and Metabolism*, *65*(2–3), 205–210.

Nielsen, J. D. (2018). *Package 'crimCV': Group-based modelling of longitudinal data*. https://CRAN.R-project.org/package=crimCV.

Nielsen, J. D., Rosenthal, J. S., Sun, Y., Day, D. M., Bevc, I., & Duchesne, T. (2014). Group-based criminal trajectory analysis using cross-validation criteria. *Communications in Statistics - Theory and Methods*, *43*(20), 4337–4356.

Nilsson, J. Å., & Svensson, M. (1993). Fledging in altricial birds: Parental manipulation or sibling competition? *Animal Behaviour*, *46*, 379–386.

Ponton, F., Elżanowski, A., Castanet, J., Chinsamy, A., Margerie, E. D., Ricqlès, A. D., & Cubo, J. (2004). Variation of the outer circumferential layer in the limb bones of birds. *Acta Ornithologica*, *39*(2), 137–140.

Prondvai, E., Kocsis, A. T., Abourachid, A., Adriaens, D., Godefroit, P., Hu, D. Y., & Butler, R. J. (2022). Radial porosity profiles: A new bone histological method for comparative developmental analysis of diametric limb bone growth. *Royal Society Open Science*, *9*, 211893.

Prondvai, E., Witten, P. E., Abourachid, A., Huysseune, A., & Adriaens, D. (2020). Extensive chondroid bone in juvenile duck limbs hints at accelerated growth mechanism in avian skeletogenesis. *Journal of Anatomy*, *236*(3), 463–473.

R Core Team. (2020). *R: A language and environment for statistical computing. R Foundation for Statistical Computing, Vienna, Austria*. http://www.R-project.org/.

Remeŝ, V., & Martin, T. E. (2002). Environmental influences on the evolution of growth and developmental rates in passerines. *Evolution*, *56*(12), 2505–2518.

Ruaux, G., Lumineau, S., & de Margerie, E. (2020). The development of flight behaviours in birds. *Proceedings of the Royal Society B: Biological Sciences*, *287*(1929), 20200668.

Santema, P., Schlicht, L., Sheldon, B. C., & Kempenaers, B. (2021). Experimental evidence that nestlings adjust their fledging time to each other in a multiparous bird. *Animal Behaviour*, *180*, 143–150.

Scanes, C. G. (Ed.). (2014). *Sturkie's Avian Physiology*. Elsevier Science & Technology.

Schneider, C. A., Rasband, W. S., & Eliceiri, K. W. (2012). NIH image to ImageJ: 25 years of image analysis. *Nature Methods*, *9*(7), 671–675.

Starck, J. M. (1993). Evolution of Avian Ontogenies. In D. M. Power (Ed.), *Current Ornithology* (pp. 275–366). Springer US.

Starck, J. M. & Sutter, E. (2000). Patterns of growth and heterochrony in moundbuilders (Megapodiidae) and fowl (Phasianidae). *Journal of Avian Biology*, *31*(4), 527–547.

Starck, M. J. & Ricklefs, R. E. (1998). Patterns of development: The altricial-precocial spectrum. In M. J. Starck, & R. E. Ricklefs (Eds.), *Avian Growth and Development. Evolution within the Altricial Precocial Spectrum* (pp. 3–30). Oxford University Press.

Thorsen, M., Innes, J., Nugent, G., & Prime, K. (2004). Parental care and growth rates of New Zealand pigeon (*Hemiphaga novaeseelandiae*) nestlings. *Notornis*, *51*, 136–140.

Unwin, D. M. & Deeming, D. C. (2019). Prenatal development in pterosaurs and its implications for their postnatal locomotory ability. *Proceedings of the Royal Society B: Biological Sciences*, *286*(1904), 20190409.

Varricchio, D. J., Balanoff, A. M., & Norell, M. A. (2015). Reidentification of avian embryonic remains from the cretaceous of Mongolia. *PLoS One*, *10*(6), e0128458.

Wang, X., Pittman, M., Zheng, X., Kaye, T. G., Falk, A. R., Hartman, S. A., & Xu, X. (2017). Basal paravian functional anatomy illuminated by high-detail body outline. *Nature Communications*, *8*(1), 14576.

Wei, X., & Zhang, Z. (2021). Femoral mechanical performance of precocial and altricial birds: a simulation study. *Avian Research*, *12*(1), 18.

Williams, B., Waddington, D., Murray, D. H., & Farquharson, C. (2004). Bone strength during growth: influence of growth rate on cortical porosity and mineralization. *Calcified Tissue International*, *74*(3), 236–245.

Xing, L., O'Connor, J. K., McKellar, R. C., Chiappe, L. M., Tseng, K., Li, G., & Bai, M. (2017). A mid-cretaceous enantiornithine (Aves) hatchling preserved in Burmese amber with unusual plumage. *Gondwana Research*, *49*, 264–277.

Yoda, K., Shiozaki, T., Shirai, M., Matsumoto, S., & Yamamoto, M. (2017). Preparation for flight: Pre-fledging exercise time is correlated with growth and fledging age in burrow-nesting seabirds. *Journal of Avian Biology*, *48*, 881–886.

Zeffer, A., Johansson, L. C., & Marmebro, Å. (2003). Functional correlation between habitat use and leg morphology in birds (Aves): habitat and leg morphology in birds (Aves). *Biological Journal of the Linnean Society*, *79*(3), 461–484.

Zeileis, A., Cribari-Neto, F., Gruen, B., Kosmidis, I., Simas, A. B., & Rocha, A. V. (2022). *Package 'betareg'*. https://CRAN.R-project.org/package=betareg

Zhou, Z. & Zhang, F. (2004). A precocial avian embryo from the lower cretaceous of China. *Science*, *306*(5696), 653.

SUPPORTING INFORMATION

Additional supporting information can be found online in the Supporting Information section at the end of this article.

How to cite this article: Prondvai, E., & Butler, R. J. (2023). Radial porosity profiles are a powerful tool for tracing locomotor maturation in developing limb bones. *Journal of Morphology*, 284, e21567. https://doi.org/10.1002/jmor.21567